Effect of Acute Heat Stress on Protein Expression and Histone Modification in The Adrenal Gland of Male Layer-Type Country Chickens

Hao-Teng Zheng
National Chung Hsing University
Zi-Xuan Zhuang
National Chung Hsing University
Chao-Jung Chen
China Medical University Hospital
Hsin-Yi Liao
China Medical University Hospital
Hung-Lin Chen
National Chung Hsing University
Huang-Chun Hsueh
National Chung Hsing University
Chih-Feng Chen
National Chung Hsing University
Shuen-Ei Chen
National Chung Hsing University
San-Yuan Huang (syhuang@dragon.nchu.edu.tw)
National Chung Hsing University

Research Article

Keywords: Acute heat stress, Adrenal gland, Proteome, Histone modification, Layer-type country chickens

Posted Date: November 25th, 2020

DOI: https://doi.org/10.21203/rs.3.rs-112324/v1

Version of Record: A version of this preprint was published at Scientific Reports on March 22nd, 2021. See the published version at https://doi.org/10.1038/s41598-021-85868-1.

Abstract

The adrenal gland responds to heat stress by epinephrine and glucocorticoid release to alleviate the adverse effects. This study investigated the effect of acute heat stress on the protein profile and histone modification in the adrenal gland of layer-type country chickens. A total of 192 30-week-old roosters were subject to acute heat stress. A resistant group and a susceptible group were identified according to body temperature change after heat stress. Adrenal glands were collected for global protein expression and histone modification analysis. The results indicated that fatty acid amide hydrolase and parathymosin were downregulated, whereas somatostatin, steroidogenic acute regulatory protein, hydroxy-δ-5-steroid dehydrogenase, 3 beta- and steroid δ-isomerase 1, and prostaglandin E synthase 3 were upregulated in the resistant group. Histone modification analysis identified 115 histone markers. The tri-methylation state of histone H3 lysine 27 (H3K27me3) was significantly more abundant in the susceptible group and showed positive crosstalk with K36me and K37me in the H3 tails. Roosters in the heat-resistant group exhibited lower hypothalamus–pituitary–adrenal axis activity but higher reactivity to maintain body temperature homeostasis. Alteration of adrenal H3K27me3 level was associated with the endocrine function of adrenal H3K27me3 and may have contributed to the thermotolerance of chickens.

Introduction

Modern chicken breeds dissipate considerable body heat and are sensitive to heat stress due to genetic selection for heightened metabolic activity and meat and egg production[1,2]. Heat stress leads to adverse alterations of behavioral, physiological, reproductive, and immunological responses, causing significant reduction in feed intake, body weight gain, egg production, and meat and egg quality[2–7]. Diminished growth, disease susceptibility, and high mortality resulting from heat stress account for a large part of the cost of poultry production throughout the world[8].

When a behavioral response fails to meet heat loss requirements under high ambient temperature, the sympathetic–adrenal–medullary axis (SAM axis) and the hypothalamus–pituitary–adrenal axis (HPA axis) are activated in poultry to compensate for the thermal imbalance[9]. Catecholamine (e.g., epinephrine and norepinephrine) and glucocorticoid (GC) release from the SAM axis and HPA axis enhance hepatic glycogenolysis and gluconeogenesis to supply more glucose and produce more energy in heat stress alleviation[10,11].

Proteomics is a powerful tool for improving genetic selection. It provides actual biomarkers for the evaluation of health status and stress tolerance in farm animals[12]. Epigenetics, highly dynamic throughout a lifetime, can affect phenotypes by altering gene expression in response to external or internal factors without altering DNA sequences[13,14]. Mechanisms of epigenetic regulation include DNA methylation, histone modification, and RNA interference[13]. Histone posttranslational modifications (HPTMs) can alter the charge state of histones, which in turn regulates chromatin structure remodeling, the access of transcription factors, and the recruitment of specific binding proteins[15]. Accordingly, environmental factors may alter HPTMs dynamically, leading to differential gene expression and translation in the plasticity and acclimatization of phenotypes.

Taiwan country chickens (TCCs) exhibit superior thermotolerance to breeds imported into Taiwan[16]. Body temperature change during heat stress is the simplest parameter to use when evaluating the adaption of chickens under thermal stress[5]. Behavioral responses to heat stress are commonly adaptive in domestic fowls, but their intensity and duration are highly variable among breeds and individuals[3]. Deciphering the genetic basis of thermotolerance in heat-resistant poultry breeds would provide information benefiting commercial chicken production in tropical areas[17]. However, a global functional genomic study in which are profiled protein expression and HPTMs of adrenal glands in response to acute heat stress in chickens has not yet been conducted. Only two studies have explored HPTMs in chicken erythrocytes through mass spectrometry (MS)[18,19]. Therefore, the aim of the present study was to investigate the effect of acute heat stress on protein expression and histone modification by using MS as a basis for delineation of the molecular mechanisms of adrenal response in the thermotolerance of domestic fowls.

Materials And Methods

Management of experimental animals

A flock of the layer-type L2 strain of TCCs, originally bred for egg production by National Chung Hsing University[64], was reared in the university farm and, at the age of 30 weeks, 197 roosters were used in the study. Animal care and use complied with guidelines approved by the Institutional Animal Care and Use Committee (IACUC) of National Chung Hsing University, Taiwan, ROC (IACUC Permit No. 104–112). The roosters were given pellet breeder diet (16.9% crude protein, 3.24% calcium, and 2,930 kcal/kg metabolizable energy) until the end of the experiment. Feed and water were provided ad libitum. Before treatment, the roosters were transferred to individual wire-floored cages in a climate chamber for an adaption period of 2 weeks under the following conditions: a 14:10-h light:dark photoperiod, 25°C, and 55% relative humidity (RH).

Conditions of acute heat stress and sample collection

A total of 192 roosters were treated with acute heat stress at 38°C and 55% RH for 4 h, as described in our previous study[65]. Five roosters were kept at 25°C and 55% RH as a control group throughout the experiment. Individual body temperature was measured by inserting an alcohol thermometer approximately 2.5 cm into the cloaca before heat treatment and at 0.5, 1, 2, 3, and 4 h into heat treatment. Blood samples were collected from the jugular vein before and after acute heat stress, and plasma was isolated and stored at −80°C until hormone analysis. The roosters were grouped by difference in body temperature between the highest value during acute heat stress and value before heat stress. This grouping resulted in definition of a resistant group ($\Delta T \leq 2.5$°C) and a susceptible group ($\Delta T \geq 6.5$°C). The control group and five roosters from each of the heat-stressed groups were sacrificed for adrenal gland collection for protein expression and histone modification analysis.

Plasma epinephrine and corticosterone analysis

Plasma epinephrine and corticosterone (CORT) levels were measured using Adrenaline Research ELISA (BA E-5100, ImmuSmol SAS, Bordeaux, France) and the Corticosterone ELISA Kit (501320, Cayman Chemical, Ann Arbor, MI, USA), respectively.

Protein sample preparation, isobaric tags for relative and absolute quantitation (iTRAQ) analysis, and fractionation of peptides

The collected adrenal glands were sliced into small pieces and lysed in O'Farrell's lysis buffer (9.5 M urea, 65 mM dithiothreitol, 2% v/v Ampholyte 3-10, and 2% NP-40). The samples were sonicated (80 W; four times for 10 s) to dissolute proteins. The homogenates were maintained at 4°C for 1 h and centrifuged at 14,000 ´*g* at 4°C for 10 min to obtain supernatants. The supernatants were mixed with 100% trichloroacetic acid (TCA) to obtain a final TCA concentration of 20% and maintained at 4°C for 1 h with shaking every 15 min. After centrifugation at 14,000*g* at 4°C for 10 min, the precipitated pellets were collected and washed with ice-cold acetone twice. The protein pellets were air-dried for 10 min and dissolved in 4 M urea solution. Protein concentrations were determined using the Bradford method with bovine serum albumin as the standard[66].

This study performed iTRAQ labeling according to the manufacturer's protocol (iTRAQ reagent multiplex kit, Applied Biosystems, Waltham, MA, USA). Five replicated protein samples from the same group were mixed and used for reduction and alkylation, which was followed by overnight digestion with trypsin. The tryptic peptides from the control, resistant, and susceptible groups were labeled with isobaric iTRAQ tags with mass 114, 115, and 116 Da, respectively. The samples were then pooled, dried using a SpeedVac evaporator (Tokyo Rikakikai Co. Ltd., Bunkyo-ku, Tokyo, Japan), and stored at −80°C until analysis.

Fractionation of the labeled peptides was performed using an ultraperformance liquid chromatography (UPLC) system (ACQUITY UPLC System, Waters, Milford, MA, USA) and a 2.1 mm × 150 mm × 1.7 μm column with a volume of 0.519 mL (ACQUITY UPLC BEH C_{18}, Waters). The mobile phase was prepared in a gradient with 10 mM ammonium bicarbonate (ABC, pH 10, mobile phase A) and 10 mM ABC/90% acetonitrile (pH 10, mobile phase B). A gradient was created with mobile phase B from 0% to 3% during min 0–5; 3% to 30% during min 5–40; 30% to 70% during min 40–55; and 70% to 0% during min 55–60. The flow rate was 0.2 μL/min. Fractions were collected in 1-min intervals for 1 h duration. Urea solutions in various fractions

were removed using C_{18} ZipTip (Merck, Darmstadt, Germany). All fractions were dried using a SpeedVac evaporator (Tokyo Rikakikai Co. Ltd.) and stored at −80°C until analysis.

Protein identification using nano-UPLC–electrospray ionization (ESI)–quadruple time-of-flight (Q-TOF)–MS/MS

A nano-LC-MS/MS system was used to analyze the tryptic peptides. The peptides were separated using an Ultimate 3000 LC RSLC nano-LC system (Dionex-Thermo Scientific, Chelmsford, MA, USA) coupled with a Q-TOF mass spectrometer (maXis impact, Bruker Daltonics Inc., Bremen, Germany). Each dried fraction was dissolved in 10 µL loading buffer (2% acetonitrile (ACN) and 0.1% FA) and injected into a C18 trapping column (Acclaim PepMap C_{18}, Dionex-Thermo Scientific) connected to a C_{18} analyst column (Acclaim PepMap C_{18}, Dionex-Thermo Scientific) for peptide separation. The labeled peptides were eluted using a linear gradient of mobile phase A (2% ACN and 0.1% FA) and mobile phase B (80% ACN and 0.1% FA) applied at a flow rate of 0.3 µL/min for 90 min. The gradient conditions were as follows: 5% to 30% mobile phase B during min 5–65; 30% to 98% mobile phase B during min 65–79, and finally, down to 10% mobile phase B within 1 min.

The mass spectrometer was operated at 50–2000 m/z at 2 Hz, and the 20 most intense ions with 420–2000 m/z in each survey scan were selected for the MS/MS experiment. MS/MS data were acquired from 50 to 2000 m/z at 5–10 Hz. The MS/MS spectra were de novo sequenced and assigned a protein ID by using PEAKS X (Bioinformatics Solutions, Waterloo, Canada) and searched against the NCBInr database (NCBInr 20180904 version) for protein identification. Protein quantification was achieved using PEAKS X with significant score ($-10\log P$) > 15, and at least one unique peptide was detected. Proteins quantified using iTRAQ as having a 1.3-fold change for a high (>1.3) or low (<0.77) level of relative abundance were considered to be differentially expressed proteins (DEPs).

Bioinformatics analysis of DEPs

The DEPs among the groups were annotated for their cellular components, biological processes, and molecular functions by using the Gene Ontology database (amigo1.geneontology.org/cgi-bin/amigo/go.cgi).

Histone sample preparation, chemical derivatization, trypsin digestion, and desalting

Histones were isolated using a modified protocol[67]. Briefly, nuclei were isolated with nuclei isolation buffer (NIB; 15 mM Tris, 60 mM KCl, 15 mM NaCl, 5 mM $MgCl_2$, 1 mM $CaCl_2$, and 250 mM sucrose and protease inhibitor cocktail tablet; pH 7.5) and 0.2% NP-40. After they had been cut into small pieces, the adrenal glands in NIB were homogenized using a homogenizer (T 10 basic ULTRA-TURRAX, IKA, Guangzhou, China), which was followed by 10 min incubation on ice. The mixture was centrifuged at 1,000 ´*g* at 4°C for 10 min, and the resultant nuclei pellets were collected. The pellets were washed with NIB twice. Histones were then acid-extracted from the isolated nuclei by using 0.2 M H_2SO_4 at 4°C for 4 h with shaking every 15 min. The histone-containing supernatants were mixed with 100% TCA to a final TCA concentration of 33% and incubated on ice for 1 h. The histone-enriched pellets were washed with ice-cold acetone/0.1% hydrochloric acid and ice-cold acetone and centrifuged to enable pellet collection. The collected pellets were air-dried and reconstituted in double-distilled water. Finally, the histones were purified through centrifugation and quantified for concentration by using the Bradford method with bovine serum albumin as the standard (Peterson, 1983). All samples were dried using a SpeedVac evaporator (Tokyo Rikakikai Co. Ltd.) and dissolved in 40 µL of 50 mM ammonium bicarbonate, which had pH 8 (concentration > 1 µg/µL). Histones were prepared for MS analysis through propionic anhydride chemical derivatization, trypsin digestion, and propionylation of histone peptides at N-termini, as was described by Sidoli et al. (2016). Then, all histone peptides were desalted with C_{18} ZipTip (Merck), dried using the SpeedVac evaporator, and finally stored at −80°C until analysis.

Identification of histone modifications by using nano-UPLC-ESI-Q-TOF-MS/MS

Nano-LC-MS/MS and the protocol for identification of histone modifications were performed as is described in section 2.5. Briefly, histone peptides dissolved in 10 µL of loading buffer were separated and eluted using a linear gradient of mobile phase A (2% ACN, 0.1% FA) and mobile phase B (80% ACN, 0.1% FA) applied at a flow rate of 0.3 µL/min for 90 min. The gradient

conditions were as follows: 10% to 40% mobile phase B at min 6–74, 40% to 99% mobile phase B at min 74.1–79, and finally, down to 10% mobile phase B within 1 min.

The MS parameters were as described in section 2.5. Label-free quantification was performed using the quantitation module of PEAKS X. Modified histone peptides were identified using PEAKS X through the following search parameters: parent mass error tolerance: 80.0 ppm; fragment mass error tolerance: 0.07 Da; enzyme: trypsin; maximum number of missed cleavages: 2; digestion mode: specific; fixed modifications: propionyl (N-term): 56.0; variable modifications: oxidation (M): 15.99, acetylation (K): 42.01, dimethylation (K): 28.03, methylation (K): 14.02, trimethylation (K): 42.05, propionyl (K): 56.03, deamidation (NQ): 0.98, propionylmethyl: 70.04; maximum number of variable PTMs per peptide: 9; reported number of peptides: 5; and data refine dependencies: 1, 4, 3, 2, 5, 6, 7, 8, 9, 10, 11, 12, 14, 13, 15, 16, 17, 19, 18, and 20. The quantification of histone modification was performed using the PEAKS DB database, which provided an overview of all peptides and histone modifications. The relative abundance of a given PTM resulting from single- or co-occurring PTMs was calculated by dividing its intensity by the sum of intensities for all modified and unmodified peptides sharing the same sequence and without missing values. Therefore, the given PTMs could have only a single datum. The quantification of each peptide of co-occurring PTMs on histone H3 was divided by the quantification of all modified and unmodified peptides to obtain a relative quantification of the histone H3 peptide and the crosstalk of PTMs on histone H3.

Statistical analysis

The concentrations of plasma epinephrine and CORT were analyzed using Student's *t* test in the Statistical Analysis System (SAS) software[68]. The normality of the body temperature changes and relative values of DEPs and HPTMs were assessed using the normality test. Normally distributed data were analyzed using the least squares means procedure, whereas nonnormally distributed data were analyzed using the Kruskal–Wallis test.

Results

Effects of acute heat stress on body temperature changes

Heat stress significantly increased body temperature ($P < 0.05$; Fig. 1). In contrast to the susceptible group, the resistant group exhibited a smaller body temperature change after heat stress ($P < 0.05$).

Fig. 1. Comparison of body temperature change in male L2 strain Taiwan country chickens (TCCs).

[a,b,c] Least squares means ± standard error (n = 5) with different superscripts indicating a significant difference between groups ($P < 0.05$).

Protein expression and annotation of DEPs in adrenal glands after acute heat stress

The iTRAQ analysis revealed that 104 of the 5,255 identified proteins were differentially expressed in the heat-stressed groups (Supplementary Table 1). Gene ontology annotation revealed that most of the DEPs were located in the cell part, intracellular and intracellular organelle (Supplementary Fig. 1). In molecular function, most of the DEPs were mainly categorized by protein binding, ion binding, and organic cyclic compound binding (Supplementary Fig. 1). Table 1 lists the 20 most vital DEPs identified in this study.

Table 1. Prominent differentially expressed proteins in the adrenal gland of male L2 strain Taiwan country chickens (TCCs) after acute heat stress.

Accession	Description	Gene symbol	Significance	Sequence coverage (%)	Peptides	Unique	Average ratio[a]		
							R/C	S/C	R/S
XP_004935335.1	Secretogranin-1 isoform X1	CHGB	34.98	45	41	41	0.76	0.68	1.12
XP_419377.1	Secretogranin-1 isoform X2	CHGB	34.98	46	41	41	0.76	0.68	1.12
XP_421330.1	Chromogranin-A isoform X1	CHGA	81	5	28	3	0.82	0.70	1.17
NP_990667.1	Somatostatin precursor	SST	20.51	42	4	4	0.88	0.65	1.35
AAS66989.1	Somatostatin, partial	SST	20.51	47	4	4	0.88	0.65	1.35
XP_422450.1	Fatty-acid amide hydrolase 1	FAAH	19.07	6	2	2	1.69	2.67	0.63
NP_990017.1	Steroidogenic acute regulatory protein, mitochondrial precursor	STAR	18.66	25	5	5	0.97	0.72	1.35
NP_990449.1	Hydroxy-δ-5-steroid dehydrogenase, 3 beta- and steroid δ-isomerase 1	HSD3B1	23.83	54	22	22	1.13	0.76	1.49
Q90955.1	Prostaglandin E synthase 3	PTGES3	24.73	32	4	4	1.63	1.00	1.63
NP_001263235.1	Prostaglandin E synthase 3	PTGES3	24.73	29	4	4	1.63	1.00	1.63
XP_015149312.1	Parathymosin	PTMS	30.36	23	3	3	0.71	1.69	0.42
XP_003642230.3	Iron-sulfur cluster assembly enzyme ISCU, mitochondrial	ISCU	19.2	27	3	3	1.57	1.03	1.52
XP_420169.3	Adrenodoxin	FDX1L	16.6	26	8	8	1.04	0.76	1.37
NP_001012910.1	Succinate–CoA ligase [ADP/GDP-forming] subunit alpha, mitochondrial	SUCLG1	16.93	31	6	6	1.61	1.04	1.55
NP_001157556.1	Selenide, water dikinase 1	SEPHS1	24.28	12	3	3	2.06	1.18	1.75
NP_990784.1	Thioredoxin	TXN	26.66	44	6	6	1.83	1.17	1.56
XP_004934466.1	Heat shock protein beta-8	HSPB8	46.03	16	3	3	0.89	2.24	0.40
NP_001010842.2	Heat shock protein beta-9	HSPB9	200	71	9	8	1.76	6.58	0.27

AAP37959.1	Heat shock protein 70	HSPA2	77.7	42	39	25	1.02	2.19	0.47
NP_001153170.1	Heat shock protein 105 kDa	HSPH1	18.84	23	17	16	0.98	1.48	0.66

[a] Only proteins with 1.3-fold change for high (>1.3) or low (< 0.77) relative protein level, as quantified using iTRAQ, were considered differentially regulated.

Validation of activity of the SAM axis and HPA axis through analysis of plasma adrenaline and CORT concentrations

No differences were discovered in actual plasma epinephrine level or its change after heat stress, but the resistant group exhibited a lower and less changed plasma CORT level than did the susceptible group ($P < 0.05$, Fig. 2).

Fig. 2. Plasma epinephrine and corticosterone concentrations of male L2 strain TCCs before and after acute heat stress. Results are expressed as mean ± standard error (n = 5).

[a,b] Superscripts indicate significant difference between groups ($P < 0.05$).

Acute heat stress modulates adrenal HPTMs

The HPTM profiles in the adrenal glands of male L2 strain TCCs were analyzed using label-free data-dependent acquisition integrated with LC-MS/MS analysis (Table 2). HPTMs analysis identified 115 histone marks on the N-terminal tails of core and linker histones, including acetylation (ac), monomethylation (me1), dimethylation (me2), and trimethylation (me3). Table 3 provides an overview of the quantified PTMs on histones H3 and H4. In contrast to the controls, the resistant roosters exhibited a significantly lower level of H3K9me, and the susceptible group had a higher level of H3K27me3 compared with the other two groups ($P < 0.05$). The relative quantification of the histone H3 peptide with single- and co-occurring PTMs is illustrated in Supplementary Fig. 2. PTMs with nearby modifications co-occurred in specific combinations and patterns to form specific crosstalk and histone codes (Fig. 3). H3K9me occurred either as a single PTM or in combination with K14ac, whereas H3K27me3 occurred either as a single PTM or in combination with K36me, K36me2, or K37me (Fig. 4A and Fig. 4B). Suppression of the level of H3K9me in the resistant group indicated negative crosstalk with K14ac, and the K14ac level was significantly lower relative to that in the control group ($P < 0.05$; Fig. 4C). The increased H3K27me3 level in the susceptible group signified positive crosstalk with K36me and K37me, but their abundance in the three groups did not differ (Fig. 4D).

Table 2. Histone posttranslational modifications (PTMs) in the adrenal gland of male L2 strain TCCs.

Histone	Acetylation	Methylation		
		Mono-	Di-	Tri-
H1	K25□K31	K25	K106	K25
H1.01	K25□K31			K25
H1.10	K25□K31			K25
H1.11L	K29□K35			K29
H2AFJ	K5	K9		K5
H2A-IV	K5	K9		K5
H2A-IV-like 3	K5	K9		K5
H2A-IV-like 2	K5	K9		K5
H2bo	K120	K116		K120
H2B-V	K120	K116		K120
H2B-VII	K120	K116		K120
H2B-VIII	K120	K116		K120
H3.3	K9□K14□K18□K23□K27□K36□K37□K79□K122	K18□K23□K27□K36□K37□K56□K79	K9□K18□K27□K36□K37□K79	K18□K27□K36□K37□K79□K122
H3	K9□K14□K18□K23□K27□K36□K37□K122	K9□K18□K23□K27□K36□K37□K56	K9□K18□K27□K36□K37	K9□K14□K18□K27□K36□K37□K122
H4	K16□K31	K31	K20□K31	K31
H5	K12□K14□K119□K120□K132□K133□K135	K12□K119□K120□K132□K133		K119□K120□K133□K135

Table 3. Summary of quantified PTMs on histones H3 and H4*.

Histone	Modification	Control	Resistant	Susceptible
H3	K9ac	15.8±1.7	13.7±0.7	15.9±1.2
	K9me	24.5±1.2[a]	20.3±0.8[b]	22.5±0.5[ab]
	K9me2	16.3±3.2	20.6±1.0	16.0±0.6
	K9me3	9.5±0.7	10.8±1.7	9.0±1.9
	K14ac	23.4±1.4	21.3±0.7	22.8±0.7
	K18ac	30.4±1.0	28.7±0.4	30.5±0.5
	K18me	1.3±0.1	1.2±0.1	1.3±0.02
	K23ac	30.8±0.8	29.1±0.8	30.5±0.5
	K23me	0.36±0.02	0.32±0.00	0.35±0.01
	K27ac	8.0±0.0	7.2±4.3	3.7±1.9
	K27me	38.9±5.0	45.1±6.5	36.4±2.8
	K27me2	14.8±6.3	14.9±7.4	10.1±4.5
	K27me3	14.1±3.0[b]	15.2±3.9[b]	30.8±5.7[a]
	K36ac	6.7±3.2	5.0±1.2	7.4±2.4
	K36me	40.7±3.1	44.7±5.5	49.4±3.6
	K36me2	7.9±1.2	8.7±0.4	8.7±0.5
	K36me3	12.6±4.7	11.9±4.3	3.7±1.1
	K37ac	9.1±2.0	14.9±3.2	12.0±0.1
	K37me	16.1±3.2	8.3±2.8	14.3±4.6
	K37me2	0.16±0.00	1.3±0.8	0
	K37me3	10.7±6.4	5.4±0.0	1.8±0.8
	K56me	1.6±0.3	2.1±0.2	12.0±0.1
	K122ac	0.33±0.02	0.32±0.01	0.31±0.02
	K122me3	0.32±0.00	0.34±0.00	0
H4	K31ac	12.4±1.7	9.9±2.8	10.5±0.5
	K31me	7.0±1.6	7.1±3.0	8.2±0.9

*The modification site, type, and relative abundance (%) of each PTM are expressed as the mean ± standard error (n = 5) without missing values. Data were analyzed using the least squares means method and Kruskal–Wallis test.

[a,b] Superscripts indicate significant difference between groups within the same PTMs ($P < 0.05$).

Fig. 3. Crosstalk of posttranslational modifications (PTMs) on histone H3 PTMs.

Distinctive types of crosstalk are indicated by connecting lines.

Fig. 4. H3K9me and H3K27me3 with distinctive crosstalk that has highly specific histone codes in the adrenal gland of different groups of male L2 strain TCCs. The relative abundance of peptides containing H3K9me and H3K27me3 is depicted in

Panels A and B, respectively, and the relative abundance of PTMs coexpressed with H3K9me and H3K27me3 are shown in Panels C and D, respectively. Results in Panel C and D are expressed as mean ± standard error (n = 5) without missing values.

[a,b] Superscripts indicate significant difference between groups within the same PTMs ($P < 0.05$).

Discussion

Chromogranin A and B (CHGA and CHGB), two major soluble proteins in adrenal medullary chromaffin granules, are implicated in the initiation and regulation of dense core granule (DCG) biogenesis in neuroendocrine cells[20]. CHGA and catecholamines are costored in DCGs and released into circulation[21]. Because catecholamine concentration is a poor marker of stress in SAM-axis activity, CHGA is considered a biomarker of target activation of the SAM axis[22]. A lack of CHGB was demonstrated to damage DCG biogenesis, leading to dysfunctional adrenal medullary chromaffin granules[20]. Disruption of DCG integrity resulted in insufficient storage of catecholamine[23]. Consistent with these results, downregulation of CHGB expression through heat stress and CHGA in the susceptible group (Table 1) may have affected DCG biogenesis, leading to decreased storage and secretion of catecholamines and thus impairment of SAM-axis activity.

Signaling of N-arachidonoylethanolamine (anandamide, AEA), which acts as a “gatekeeper,” has an inhibitory role in the activity and regulatory steady state of the HPA axis to maintain baseline GC level under normal conditions, and removal of this AEA tone by fatty acid amide hydrolase (FAAH) in response to stress results in activation of the HPA axis[24–26]. Thus, upregulation of FAAH in the heat-stressed groups (Table 1) may have degraded the AEA level and promoted the secretion of GC from the adrenal glands to alleviate the acute heat stress. Somatostatin (STT) also plays an inhibitory role in the secretion of multiple hormones and bioactive peptides in the HPA axis[27–29]. Therefore, upregulated STT expression and downregulation of FAAH in the resistant group (Table 1) compared with the susceptible group may reflect quick adaption by the HPA axis in response to acute heat stress.

The secretion of adrenal CORT is regulated in a pulsatile manner through fluctuation of cellular transcript levels of steroidogenic genes including steroidogenic acute regulatory protein (STAR) and 3β-hydroxysteroid dehydrogenase/δ(5)-δ(4) isomerase type I (HSD3B1) in response to the stimulation of an adrenocorticotropic hormone pulse[30–32]. The physiological actions of GC are mediated by the glucocorticoid receptor (GR)[33]. When the GC level is low, the GR is deactivated by binding with molecular chaperones including heat shock protein 90 and prostaglandin E synthase 3 (PTGES3) in cytoplasm[34]. Parathymosin functions as a critical coactivator of GR for downstream target gene expression[35,36]. Red junglefowls, the primary ancestor of domestic fowls, exhibit higher HPA axis reactivity than do modern White Leghorn layers[37,38]. Red junglefowls quickly respond to acute stress with high CORT secretion and adapt to the stress with a rapid decline of CORT secretion accompanied by a quick change in STAR expression. Because newly synthesized steroidogenic proteins are involved in the rapid synthesis of GC following each pulse of adrenocorticotropic hormone, intracellular stores of steroidogenic proteins are depleted for more pulsatile secretion of GC[31,39]. The differences between red junglefowls and White Leghorns in HPA axis reactivity to stress reflect the genetic effects of domestication and selection; differing gene expression (Table 1), HPA axis activity (Fig. 2), and body temperature change (<2.5°C vs. >6.5°C; Fig. 1) between the resistant and susceptible roosters indicate intrinsic heterogeneity in the genetics of the native chickens. In contrast to the susceptible roosters, the resistant roosters had a minor increase in body temperature by heat stress in association with unchanged plasma CORT level and adrenal STAR and HSD3B1 expression but significantly upregulated PTGES3 and downregulated parathymosin expression, which suggested rapid physiological regulation in adaption to heat stress.

Iron–sulfur cluster assembly enzyme (ISCU) is the scaffold protein that participates in the first step of iron–sulfur cluster formation in mitochondrial respiratory complexes[40,41]. Adrenodoxin promotes iron–sulfur cluster formation and participates in adrenal steroidogenesis[40,42]. Succinate-CoA ligase (SUCLG1) regulates mitochondrial DNA synthesis through nucleotide synthesis and transportation for the production of key subunits of mitochondrial respiratory chain complexes[43,44]. Higher ISCU, adrenodoxin, and SUCLG1 expression levels in the resistant group than in the susceptible group (Table 1) may indicate more

sufficient mitochondrial function for ATP supply to meet the need for functional adrenal glands for heat dissipation. Greater ATP production thus promotes cellular oxidative stress due to leakage of reactive oxygen species from the mitochondria, leading to upregulation of selenide, water dikinase 1, and thioredoxin in cellular antioxidative defense for achieving cellular redox balance[45–47]. In contrast to that of the susceptible group, the expression of heat shock proteins, including HSPB8, HSPB9, HSP70, and HSP105, in the resistant roosters was lower (Table 1), suggesting less oxidative damage in the adrenal gland resulting from heat stress[48].

Cell responses to stimuli depend on the regulation of genetic and epigenetic homeostasis and a dynamic balance of stability and reversibility in gene expression patterns[14]. Therefore, dynamic changes in HPTMs are closely associated with cellular physiological state[15]. Histones H3 and H4 are the best characterized and common as well as the most highly conserved histones, suggesting that they play a prominent regulatory role in chromatin formation[49,50]. Histone modification studies have quantified 26 PTMs in histones H3 and H4 (Table 3) under acute heat stress. H3K9me is involved in transcriptional activation[15], whereas H3K27me3 is associated with facultative heterochromatin for gene repression[51]. H3K27me3 is among the most studied HPTM[52], and a change in H3K27me3 may be involved in the thermotolerance of male L2 strain TCCs. Previous studies have reported the effect of Marek's disease on a genome-wide map of H3K27me3 in the immune response of the spleen, thymus, and bursa of Fabricius in chickens[53–55]. Therefore, studies using chromatin immunoprecipitation followed by sequencing (ChIP-seq) technology to investigate adrenal H3K9me and H3K27me3 regulation in specific gene expression and thermotolerance phenotypes are underway.

Histones can be reversibly modified at multiple sites by specific histone-modifying enzymes[56]. Moreover, PTMs have diverse functions and regulate other PTMs leading to regulatory crosstalk[57]. Crosstalk can occur on the same histone molecule, between histones, or across nucleosomes; thus, one PTM can affect the occurrence of one or more subsequent PTMs through the interaction of "writers," "erasers," and "readers"[57]. The combination of these specific HPTMs through crosstalk constitutes an epigenetic code that acts as an information-rich signaling platform to recruit downstream "readers" or "effectors" or to directly regulate nucleosomal structure for specific gene transcription and cellular phenotypes[15,58,59]. Epigenetic code is much more significant than the contribution of any single PTM. It elucidates the mechanisms of crosstalk within and between histones in nucleosomes[56]. The length of the peptides generated through propionic anhydride derivatization and trypsin digestion does not give an overview of the entire protein sequence and its modification state, but crosstalk on the same histone can be observed for nearby modifications. The crosstalk of combinatorial PTMs on histone H3 (Fig. 3) in the adrenal gland of the chickens in this study was specific and may convey distinct biological functions and epigenetic codes. The abundance of H3K9me occurred either as a single PTM or in combination with K14ac, and the abundance of H3K27me3 occurred either as a single PTM or in combination with K36me, K36me2, or K37me (Fig. 4A and Fig. 4B). Codependent PTMs within the same histone are typically described as a positive crosstalk, whereas mutually exclusive PTMs are described as a negative crosstalk[60]. The decreased abundance of H3K9me in the resistant roosters indicated a negative crosstalk with K14ac, and the increased abundance of H3K27me3 in susceptible roosters signified a positive crosstalk with K36me and K37me (Fig. 4C and Fig. 4D). Therefore, the interplay of these combinatorial PTMs may play a role in the regulation of the intensity and duration of acute heat stress in the adrenal gland of male L2 strain TCCs and deserves further exploration.

Cell type-specific GR actions have been demonstrated to depend on epigenetics, nucleosome structure, and DNA accessibility[61–63]. Euchromatin, or relaxed chromatin, is transcriptionally active and enriched for active HPTMs (e.g., H3K4me3), whereas heterochromatin or compacted chromatin is transcriptionally repressive and enriched for repressive HPTMs (e.g., H3K27me3)[52]. Therefore, the complex of GC and GR can bind to glucocorticoid response elements and initiate GR-dependent transcription in euchromatin, but it is denied access to the GC response elements in heterochromatin[61,63]. In contrast to the other groups, the higher level of adrenal H3K27me3 in the susceptible group (Table 3) may indicate a more inaccessible conformation of chromatin remodeling for the access of specific transcription factors.

In summary, heat stress resulted in 104 DEPs in the adrenal glands of male L2 strain TCCs, and histone modification analysis identified 115 PTMs. Functional pathway analysis indicated that compared with the susceptible group, the resistant group had

higher HPA axis reactivity, mitochondrial function, and antioxidant capacity in the adrenal gland, maintaining homeostasis of body temperature under acute heat stress. The susceptible group exhibited higher HPA axis activity, but its adrenal chromatin remodeling was constituted mainly in the form of heterochromatin as an increased abundance of H3K27me3. Therefore, dysfunctional maintenance of the homeostasis of body temperature in the susceptible roosters may have caused excessive HPA axis activity, leading to exhausted adrenal function. The alteration of adrenal H3K27me3 level was associated with adrenal functionality in the thermotolerance of the TCCs. The interplay between HPTMs and phenotypes requires further investigation using technologies such as ChIP-seq.

Declarations

Acknowledgements

This study was financially supported by the Ministry of Science and Technology (contract nos. MOST105-2321-B-005-014, MOST106-2321-B-005-007 and MOST107-2313-B-005-034), and The iEGG and Animal Biotechnology Center from The Future Areas Research Center Program within the framework of the Higher Education Sprout Project by the Ministry of Education in Taiwan (contract no. 108-S-0023).

Author Contributions Statement

HTZ ZXZ CJC CFC SEC SYH conceived and designed the experiments. HTZ ZXZ HYL HLC HCH performed the experiments. HTZ CJC HYL analyzed the data. CJC CFC SEC SYH contributed reagents/materials/analysis tools. HTZ SEC SYH wrote the paper. All authors reviewed the manuscript.

Competing financial interests

The authors declare no competing financial interests.

References

1. Deeb, N. & Cahanerm, A. Genotype-by-environment interaction with broiler genotypes differing in growth rate. 3. Growth rate and water consumption of broiler progeny from weight-selected versus non selected parents under normal and high ambient temperatures. *Poult. Sci.* **81,** 293–301 (2002).
2. Pawar, S. S. *et al*. Assessing and mitigating the impact of heat stress in poultry. Adv. *Anim. Vet. Sci*. 4, 332–341 (2016).
3. Lara, L. J. & Rostagno, M. H. Impact of heat stress on poultry production. *Animals* **3,** 356–369 (2013).
4. Cheng, C. Y. *et al*. Functional genomics study of acute heat stress response in the small yellow follicles of layer-type chickens. *Sci. Rep.* **8,** 1320 (2018).
5. Farag, M. R. & Alagawany, M. Physiological alterations of poultry to the high environmental temperature. *J. Therm. Biol.* **76,** 101–106 (2018).
6. Tu, W. L. *et al*. Annotation of differential protein expression in the hypothalami of layer-type Taiwan country chickens in response to acute heat stress. *J. Therm. Biol*. **77,** 157–172 (2018).
7. Wang, S. H. *et al*. Acute heat stress changes protein expression in the testes of a broiler-type strain of Taiwan country chickens. *Anim. Biotechnol*. **30,** 129–145 (2018).
8. Mishra, B. & Jha, R. Oxidative stress in the poultry gut: Potential challenges and interventions. *Front. Vet. Sci*. **6,** 60 (2019).
9. Calefi, A. S., Quinteiro-Filho, W. M., Ferreira, A. J. P. & Palermo-Neto, J. Neuroimmunomodulation and heat stress in poultry. *Worlds Poult. Sci. J*. **73,** 493–504 (2017).
10. Barth, E. *et al*. Glucose metabolism and catecholamines. *Crit. Care. Med*. **35,** 508–518 (2007).
11. Opata, A. A., Cheesman, K. C. & Geer, E. B. *The Hypothalamic Pituitary Adrenal Axis in Health and Disease: Cushing's Syndrome and Beyond. Page 3 in Glucocorticoid Regulation of Body Composition and Metabolism* (Springer, Cham, 2016).

12. Boschetti, E., Hernandez-Castellano, L. E. & Righetti, P. G. Progress in farm animal proteomics: The contribution of combinatorial peptide ligand libraries. *J. Proteomics*. **197,** 1–13 (2019).
13. Kim, G. H., Ryan, J. J., Marsboom, G. & Archer, S. L. Epigenetic mechanisms of pulmonary hypertension. *Pulm. Circ.* **1,** 347–356 (2011).
14. Ibeagha-Awemu, E. M. & Zhao, X. Epigenetic marks: Regulators of livestock phenotypes and conceivable sources of missing variation in livestock improvement programs. *Front. Genet.* **6,** 302 (2015).
15. Huang, H., Lin, S., Garcia, B. A. & Zhao, Y. Quantitative proteomic analysis of histone modifications. *Chem. Rev.* **115,** 2376–2418 (2015).
16. Yeh, C.C. Effect of acute heat stress on the blood characteristics of Taiwan country chickens and broilers. *J. Chin. Soc. Anim. Sci.* **21,** 57–66 (1992).
17. Nawab, A. *et al*. Heat stress in poultry production: Mitigation strategies to overcome the future challenges facing the global poultry industry. *J. Therm. Biol.* **78,** 131–139 (2018).
18. Sarg, B. *et al*. Identification of novel post-translational modifications in linker histones from chicken erythrocytes. *J. Proteomics*. **113,** 162–177 (2015).
19. Wu, H., Xiao, K. & Tian, Z. Top-down characterization of chicken core histones. *J. Proteomics*. **184,** 34–38 (2018).
20. Kim, T. & Loh, Y. P. Chromogranin A: A surprising link between granule biogenesis and hypertension. *J. Clin. Invest.* **115,** 1711–1713 (2005).
21. Valdiglesias, V. *et al*. Is salivary chromogranin A a valid psychological stress biomarker during sensory stimulation in people with advanced dementia? *J. Alzheimers Dis.* **55,** 1509–1517 (2017).
22. Escribano, D., *et al*. Salivary biomarkers to monitor stress due to aggression after weaning in piglets. *Res. Vet. Sci.* **123,** 178–183 (2019).
23. Pasqua, T. *et al*. Impact of chromogranin A deficiency on catecholamine storage, catecholamine granule morphology and chromaffin cell energy metabolism in vivo. *Cell Tissue Res.* **363,** 693–712 (2016).
24. Hill, M. N. & McEwen, B. S. Involvement of the endocannabinoid system in the neurobehavioural effects of stress and glucocorticoids. *Prog. Neuropsychopharmacol. Biol. Psychiatry*. **34,** 791–797 (2010).
25. Crowe, M. S., Nass, S. R., Gabella, K. M. & Kinsey, S. G. The endocannabinoid system modulates stress, emotionality, and inflammation. *Brain Behav. Immun.* **42,** 1–5 (2014).
26. Lee, T. T. & Gorzalka, B. B. Evidence for a role of adolescent endocannabinoid signaling in regulating HPA axis stress responsivity and emotional behavior development. *Int. Rev. Neurobiol.* **125,** 49–84 (2015).
27. Bram, Z. *et al*. Does somatostatin have a role in the regulation of cortisol secretion in primary pigmented nodular adrenocortical disease (PPNAD)? A clinical and in vitro investigation. *J. Clin. Endocrinol. Metab.* **99,** 891–901 (2014).
28. Lin, L. C., & Sibille, E. Somatostatin, neuronal vulnerability and behavioral emotionality. *Mol. Psychiatry*. **20,** 377–387 (2015).
29. Stengel, A. & Tache, Y. F. Activation of brain somatostatin signaling suppresses CRF receptor-mediated stress response. *Front. Neurosci.* **11,** 231 (2017).
30. Payne, A. H. & Hales, D. B. Overview of steroidogenic enzymes in the pathway from cholesterol to active steroid hormones. *Endocr. Rev.* **25,** 947–970 (2004).
31. Spiga, F., Walker, J. J., Terry, J. R. & Lightman, S. L. HPA axis-rhythms. *Comp. Physiol.* **4,** 1273–1298 (2014).
32. Hettel, D. & Sharifi, N. HSD3B1 status as a biomarker of androgen deprivation resistance and implications for prostate cancer. *Nat. Rev. Urol.* **15,** 191–196 (2018).
33. Gross, K. L., Lu, N. Z. & Cidlowski, J. A. Molecular mechanisms regulating glucocorticoid sensitivity and resistance. *Mol. Cell. Endocrinol.* **300,** 7–16 (2009).
34. Schoneveld, O. J., Gaemers, I. C. & Lamers, W. H. Mechanisms of glucocorticoid signalling. *Biochim. Biophys. Acta.* **1680,** 114–128 (2004).

35. Okamoto, K. & Isohashi, F. Macromolecular translocation inhibitor II (Zn^{2+}-binding protein, parathymosin) interacts with the glucocorticoid receptor and enhances transcription in vivo. *J. Biol. Chem.* **280,** 36986–36993 (2005).
36. Okamoto, K. *et al*. A small nuclear acidic protein (MTI-II, Zn^{2+} binding protein, parathymosin) that inhibits transcriptional activity of NF-κB and its potential application to antiinflammatory drugs. *Endocrinology* **157,** 4973–4986 (2016).
37. Ericsson, M., Fallahsharoudi, A., Bergquist, J., Kushnir, M. M. & Jensen, P. Domestication effects on behavioural and hormonal responses to acute stress in chickens. *Physiol. Behav*. **133,** 161–169 (2014).
38. Fallahsharoudi, A. *et al*. Domestication effects on stress induced steroid secretion and adrenal gene expression in chickens. *Sci. Rep.* **5,** 15345 (2015).
39. Artemenko, I. P., Zhao, D., Hales, D. B., Hales, K. H. & Jefcoate, C. R. Mitochondrial processing of newly synthesized steroidogenic acute regulatory protein (StAR), but not total StAR, mediates cholesterol transfer to cytochrome P450 side chain cleavage enzyme in adrenal cells. *J. Biol. Chem.* **276,** 46583–46596 (2001).
40. Spiegel, R. *et al*. Deleterious mutation in FDX1L gene is associated with a novel mitochondrial muscle myopathy. *Eur. J. Hum. Genet.* **22,** 902–906 (2014).
41. Cai, K., Tonelli, M., Frederick, R. O. & Markley, J. L. Human mitochondrial ferredoxin 1 (FDX1) and ferredoxin 2 (FDX2) both bind cysteine desulfurase and donate electrons for iron-sulfur cluster biosynthesis. *Biochemistry* **56,** 487–499 (2017).
42. Sheftel, A. D. *et al*. Humans possess two mitochondrial ferredoxins, FDX1 and FDX2, with distinct roles in steroidogenesis, heme, and Fe/S cluster biosynthesis. *Proc. Natl. Acad. Sci. U.S.A.* **107,** 11775–11780 (2010).
43. El-Hattab, A. W. & Scaglia, F. Mitochondrial DNA depletion syndromes: Review and updates of genetic basis, manifestations, and therapeutic options. *Neurotherapeutics*. **10,** 186–198 (2013).
44. Maalej, M. *et al*. Clinical, molecular, and computational analysis in two cases with mitochondrial encephalomyopathy associated with SUCLG1 mutation in a consanguineous family. *Biochem. Biophys. Res. Commun.* **495,** 1730–1737 (2018).
45. Na, J. *et al*. Selenophosphate synthetase 1 and its role in redox homeostasis, defense and proliferation. *Free Radic. Biol. Med.* **127,** 190–197 (2018).
46. Lee, S., Kim, S. M. & Lee, R. T. Thioredoxin and thioredoxin target proteins: From molecular mechanisms to functional significance. *Antioxid. Redox Signal.* **18,** 1165–1207 (2013).
47. Zhang, J., Li, X., Han, X., Liu, R. & Fang, J. Targeting the thioredoxin system for cancer therapy. *Trends Pharmacol. Sci.* **38,** 794–808 (2017).
48. Slimen, I. B. *et al*. Reactive oxygen species, heat stress and oxidative-induced mitochondrial damage. A review. *Int. J. Hyperthermia*. **30,** 513–523 (2014).
49. Hyland, E. M. *et al*. Insights into the role of histone H3 and histone H4 core modifiable residues in *Saccharomyces Cerevisiae*. *Mol. Cell Biol.* **25,** 10060–10070 (2005).
50. Postberg, J., Forcob, S., Chang, W. J. & Lipps, H. J. The evolutionary history of histone H3 suggests a deep eukaryotic root of chromatin modifying mechanisms. *BMC Evol. Biol.* **10,** 259 (2010).
51. Corso-Diaz, X., Jaeger, C., Chaitankar, V. & Swaroop, A. Epigenetic control of gene regulation during development and disease: A view from the retina. *Prog. Retin. Eye Res.* **65,** 1–27 (2018).
52. David, S.-A. *et al*. Genome-wide epigenetic studies in chicken: A review. *Epigenomes* **1,** 20 (2017).
53. Luo, J. *et al*. Histone methylation analysis and pathway predictions in chickens after MDV infection. *PLoS ONE* **7,** e41849 (2012).
54. Mitra, A. *et al*. Marek's disease virus infection induces widespread differential chromatin marks in inbred chicken lines. *BMC Genomics* **13,** 557 (2012).
55. Mitra, A. *et al*. Histone modifications induced by MDV infection at early cytolytic and latency phases. *BMC Genomics* **16,** 311 (2015).
56. Sidoli, S., Cheng, L. & Jensen, O. N. Proteomics in chromatin biology and epigenetics: Elucidation of post-translational modifications of histone proteins by mass spectrometry. *J. Proteomics*. **75,** 3419–3433 (2012).

57. Latham, J. A. & Dent, S. Y. Cross-regulation of histone modifications. *Nat. Struct. Mol. Biol.* **14,** 1017–1024 (2007).
58. Chi, P., Allis, C. D. & Wang, G. G. Covalent histone modifications–miswritten, misinterpreted and mis-erased in human cancers. *Nat. Rev. Cancer.* **10,** 457–469 (2010).
59. Young, N. L., Dimaggio, P. A. & Garcia, B. A. The significance, development and progress of high-throughput combinatorial histone code analysis. *Cell. Mol. Life Sci.* **67,** 3983–4000 (2010).
60. Schwammle, V. *et al.* Systems level analysis of histone H3 post-translational modifications (PTMs) reveals features of PTM crosstalk in chromatin regulation. *Mol. Cell. Proteomics* **15,** 2715–2729 (2016).
61. Knutson, S. K. *et al.* Synergistic anti-tumor activity of EZH2 inhibitors and glucocorticoid receptor agonists in models of germinal center non-hodgkin lymphomas. *PLoS ONE* **9,** e111840 (2014).
62. Greulich, F., Hemmer, M. C. Rollins, D. A., Rogatsky, I. & Uhlenhaut, N. H. There goes the neighborhood: Assembly of transcriptional complexes during the regulation of metabolism and inflammation by the glucocorticoid receptor. *Steroids* **114,** 7–15 (2016).
63. Misale, M. S., Witek Janusek, L., Tell, D. & Mathews, H. L. Chromatin organization as an indicator of glucocorticoid induced natural killer cell dysfunction. *Brain Behav. Immun.* **67,** 279–289 (2018).
64. Yang, K. T. *et al.* Expressed transcripts associated with high rates of egg production in chicken ovarian follicles. *Mol. Cell. Probes.* **22,** 47–54 (2008).
65. Zhuang, Z. X., Chen, S. E., Chen, C. F., Lin, E. C. & Huang S. Y. Genomic regions and pathways associated with thermotolerance in layer-type strain Taiwan indigenous chickens. *J. Therm. Biol.* **88,** 102486 (2020).
66. Peterson, G. L. Determination of total protein. *Methods Enzymol.* **91,** 95–119 (1983).
67. Sidoli, S., Bhanu, N. V., Karch, K. R., Wang, X. & Garcia, B. A. Complete workflow for analysis of histone post-translational modifications using bottom-up mass spectrometry: From histone extraction to data analysis. *J. Vis. Exp.* **111,** e54112 (2016).
68. SAS Institute Inc. SAS/STAT 9.2 User's Guide. (SAS Institute Inc, Cary, 2013).

Figures

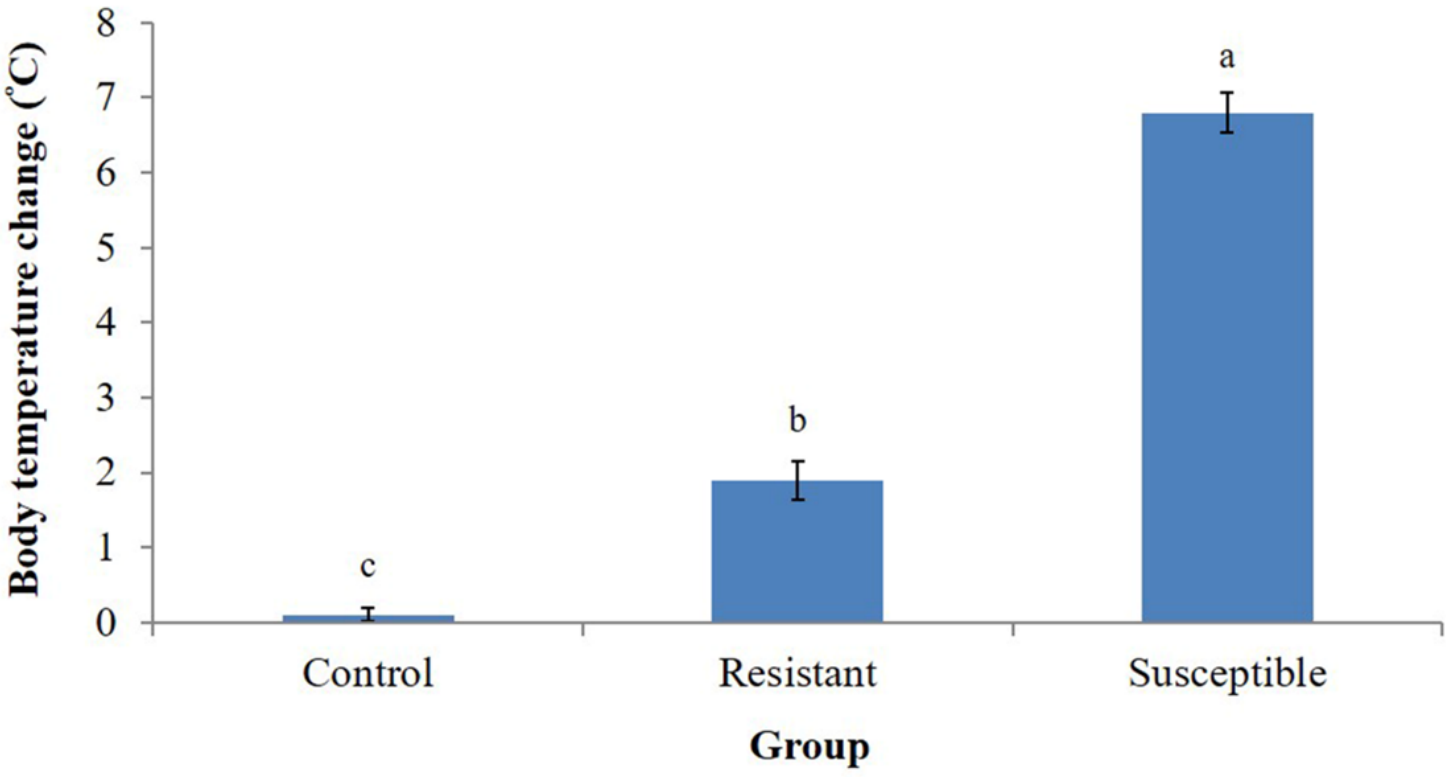

Figure 1

Comparison of body temperature change in male L2 strain Taiwan country chickens (TCCs). a,b,c Least squares means ± standard error (n = 5) with different superscripts indicating a significant difference between groups (P < 0.05).

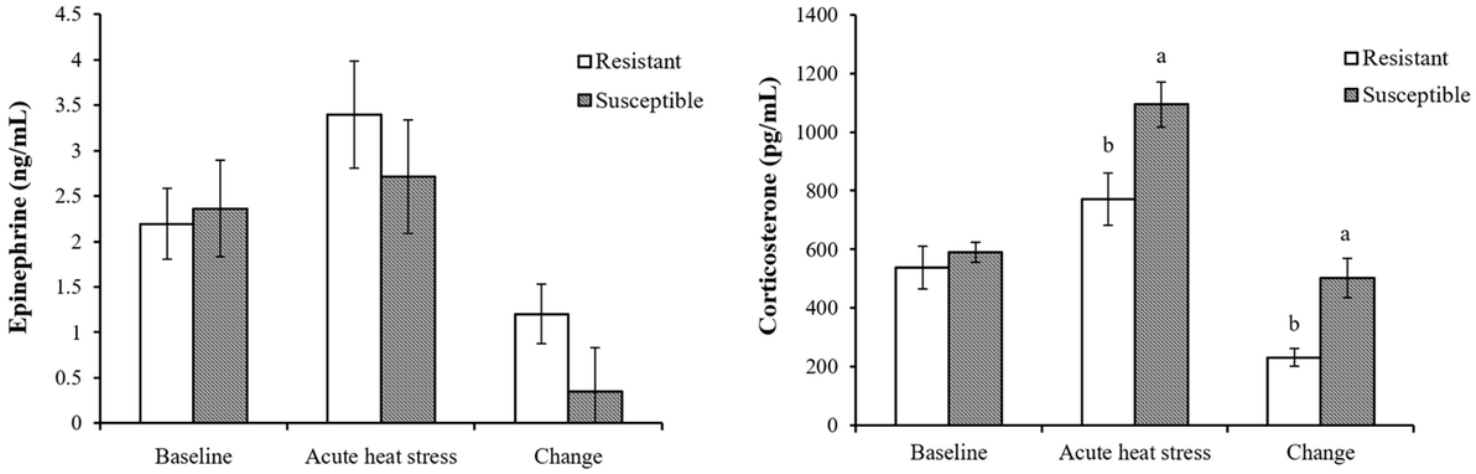

Figure 2

Plasma epinephrine and corticosterone concentrations of male L2 strain TCCs before and after acute heat stress. Results are expressed as mean ± standard error (n = 5). a,b Superscripts indicate significant difference between groups (P < 0.05).

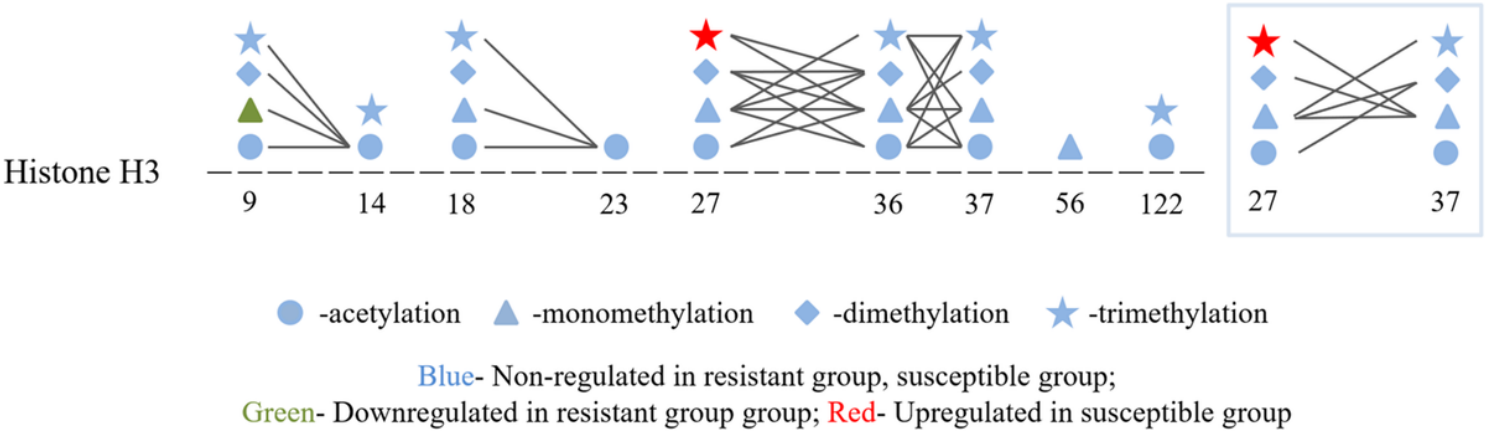

Figure 3

Crosstalk of posttranslational modifications (PTMs) on histone H3 PTMs. Distinctive types of crosstalk are indicated by connecting lines.

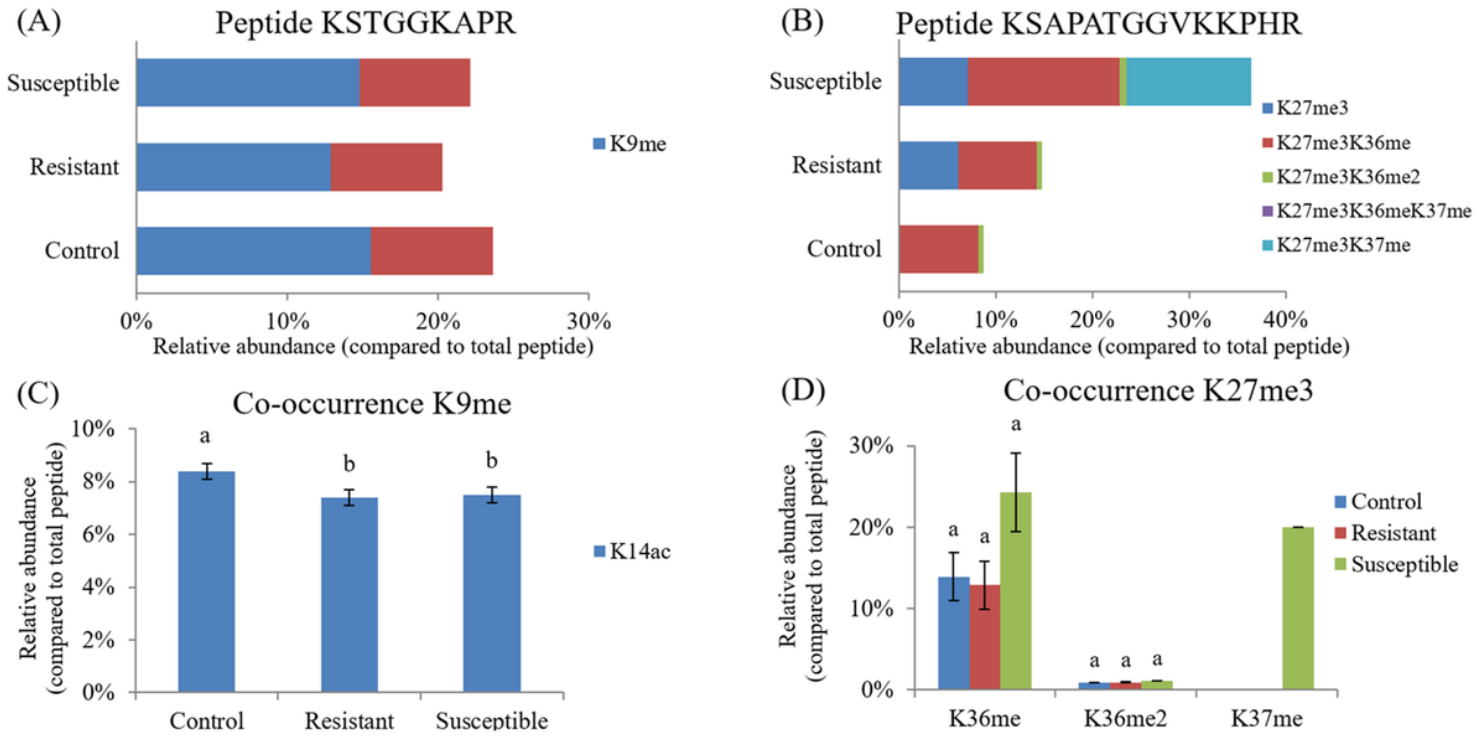

Figure 4

H3K9me and H3K27me3 with distinctive crosstalk that has highly specific histone codes in the adrenal gland of different groups of male L2 strain TCCs. The relative abundance of peptides containing H3K9me and H3K27me3 is depicted in Panels A and B, respectively, and the relative abundance of PTMs coexpressed with H3K9me and H3K27me3 are shown in Panels C and D, respectively. Results in Panel C and D are expressed as mean ± standard error (n = 5) without missing values. a,b Superscripts indicate significant difference between groups within the same PTMs ($P < 0.05$).

Supplementary Files

This is a list of supplementary files associated with this preprint. Click to download.

- SupplementaryTableS1.docx
- Supplementaryinformation.pdf